

Fumarates Promote Cytoprotection of Central Nervous System Cells Against Oxidative Stress via the Nrf2 Pathway

Robert H. Scannevin, Sowmya Chollate, Mi-young Jung, Melanie Shackett, Hiral Patel, Pradeep Bista, Wei-ke Zeng, Sarah Ryan, Masayuki Yamamoto, Matvey Lukashev and Kenneth J. Rhodes

Biogen Idec, Weston Massachusetts, USA (R.H.S, S.C., M-Y.J., M.S., H.P., P.B., W.Z., S.R., M.L., K.J.R) and Department of Medical Biochemistry, Tohoku University Graduate School of Medicine, Sendai, Japan (M.Y.).

Running Title: Nrf2-Dependent Cytoprotection Against Oxidative Stress

Corresponding Author: Robert H .Scannevin

Biogen Idec

14 Cambridge Center

Cambridge, MA 02142

Phone: (617) 914-1189

Fax: (617) 679-3200

Email: robert.scannevin@biogenidec.com

Text Pages: 35

Figures: 7

Tables: 1

References: 40

Abstract Words: 250 (250 maximum)

Introduction Words: 704 (750 maximum)

Discussion Words: 953 (1500 maximum)

Abbreviations

MS, multiple sclerosis; CNS, central nervous system; DMF, dimethyl fumarate; MMF, monomethyl fumarate; EAE, experimental autoimmune encephalomyelitis; qPCR, quantitative PCR; NQO1, nicotinamide adenine dinucleotide phosphate dehydrogenase (quinone 1); Akr1b8, aldo-keto reductase family 1, member B8;

HO1, heme-oxygenase 1; GCLC, glutamate-cysteine ligase catalytic subunit;
DMSO, dimethyl sulfoxide; hOPC, human oligodendrocyte precursor cell; hNeur,
human neuron; rOPC, rat oligodendrocyte precursor cell; DAPI, 4',6 diamidino-2-
phenylindole; GSH, glutathione; TMRE, tetramethyl rhodamine ester; RFU,
relative fluorescence units; siRNA, small interfering RNA; HDAC, histone
deacetylase

Recommended Section Assignment: Neuropharmacology

Abstract

Oxidative stress is central to the pathology of several neurodegenerative diseases, including multiple sclerosis (MS), and therapeutics designed to enhance antioxidant potential could have clinical value. The objective of this study was to characterize the potential direct neuroprotective effects of dimethyl fumarate (DMF) and its primary metabolite monomethyl fumarate (MMF) on cellular resistance to oxidative damage in primary cultures of central nervous system (CNS) cells and further explore the dependence and function of the nuclear factor (erythroid-derived 2)-like 2 (Nrf2) pathway in this process. Treatment of animals or primary cultures of CNS cells with DMF or MMF resulted in increased nuclear levels of active Nrf2, with subsequent upregulation of canonical antioxidant target genes. DMF-dependent upregulation of antioxidant genes in vivo was lost in mice lacking Nrf2 (Nrf2^{-/-}). DMF or MMF treatment increased cellular redox potential, glutathione, ATP levels and mitochondrial membrane potential in a concentration-dependent manner. Treating astrocytes or neurons with DMF or MMF also significantly improved cell viability after toxic oxidative challenge in a concentration-dependent manner. This effect on viability was lost in cells that had eliminated or reduced Nrf2. These data suggest that DMF and MMF are cytoprotective for neurons and astrocytes against oxidative stress-induced cellular injury and loss, potentially via upregulation of an Nrf2-dependent antioxidant response. These data also suggest DMF and MMF may function through improving mitochondrial function. The clinical utility of DMF in

multiple sclerosis is being explored through phase III trials with BG-12, which is an oral therapeutic containing DMF as the active ingredient.

Introduction

Free radicals exert significant oxidative stress on tissues and cells and are implicated as contributing factors to the pathology of diverse neurodegenerative disorders such as multiple sclerosis (MS), amyotrophic lateral sclerosis, Huntington's, Parkinson's and Alzheimer's disease. The post-mitotic cells that reside in the central nervous system (CNS) have an inherently low capacity for mitigating oxidative stress, and are highly susceptible to its damaging effects on DNA, proteins and lipids (Hardingham and Lipton 2010). Current therapeutic approaches typically target molecular pathways associated with individual diseases or, in the case of MS, broadly impact immune function. However, little has been done to mitigate the common pathological feature of oxidative stress.

All cells have an intrinsic mechanism for combating reactive oxygen species (ROS) that is dynamically controlled through the actions of Nrf2, a transcription factor that is the principal regulator of the phase II cellular antioxidant response (Nguyen et al., 2003). Nrf2 is normally sequestered in the cytoplasm through interaction with kelch-like erythroid cell-derived protein with CNC homology -associated protein 1 (Keap1), which results in constitutive protein ubiquitination and proteosomal degradation. However, excessive ROS, or treatment with electrophilic compounds, results in modification of Keap1 such that Nrf2 is no longer constitutively degraded (Itoh et al., 2004; Li and Kong 2009; Linker et al., 2011). This results in the accumulation of Nrf2 in cellular nuclei and

enhanced transcription of a host of antioxidant and detoxification genes (Kwak et al., 2003; Lee et al., 2003).

Electrophilic compounds have been shown to induce activation of the Nrf2 pathway and many of them, including carnosine (Calabrese et al., 2005), tert-butylhydroquinone (Li et al., 2005), the synthetic triterpenoid CDDO-methyl amide (Tran et al., 2008; Yang et al., 2009), sulforaphane (Soane et al., 2010), and 1,5-dicaffeoylquinic acid (Cao et al., 2010), have demonstrated *in vitro* cytoprotective responses against oxidative and inflammatory stress in treated neuronal cells. By using these types of compounds or via genetic overexpression, the neuroprotective effects of Nrf2 pathway activation have been investigated in animal models of various neurodegenerative disorders, such as Alzheimer's disease (Dumont et al., 2009), Parkinson's disease (Jakel et al., 2007; Chen et al., 2009; Yang et al., 2009), amyotrophic lateral sclerosis (Vargas et al., 2008; Neymotin et al., 2011) and Huntington's disease (Stack et al., 2010).

Recent studies have demonstrated that the fumaric acid ester, dimethyl fumarate (DMF), and its primary metabolite monomethyl fumarate (MMF) (Table 1), were able to activate the Nrf2 pathway and induced expression of antioxidant proteins (Lin et al., 2011) and that administration of MMF could protect motor neurons and astrocytes against H₂O₂-induced oxidative stress (Linker et al., 2011). These results may point to an underlying functional cellular substrate for the neuroprotective response observed in mouse experimental autoimmune encephalomyelitis (EAE), in which DMF treatment, in comparison with vehicle controls, reduced oxidative damage and consequential nerve fiber demyelination,

resulting in greater axonal preservation and improved motor function (Schilling et al., 2006; Linker et al., 2011). The therapeutic relevance of the Nrf2 pathway has been shown by the lack of response to DMF in Nrf2^{-/-} EAE models (Linker et al., 2011). DMF has also been shown to improve lifespan, reduce behavioral deficits, and preserve striatal and motor cortex neurons in two different genetic models of Huntington's disease (Ellrichmann et al., 2011), suggesting it may have broad neuroprotective properties.

The results from the present study have demonstrated that DMF induced a broad pharmacodynamic response after oral dosing in mice, and the upregulation of this response was dependent upon Nrf2. Primary cultures of neurons, astrocytes and oligodendrocyte precursor cells were utilized to demonstrate the DMF- and MMF-dependent stabilization of Nrf2 in different CNS cell types, indicating the relevance of these compounds in treating diseases that result in the degeneration of CNS cells. The functional consequence of Nrf2 activation was characterized in astrocytes and neurons challenged with toxic oxidative stress, in which DMF and MMF promoted improved viability in an Nrf2-dependent manner. A potential functional mechanism by which cytoprotection may be conferred was identified through an upregulation of the cellular antioxidant response and preservation of mitochondrial function. These studies expand upon the potential mechanism of action for BG-12, a second generation fumarate containing DMF, which has demonstrated promising efficacy in phase II and phase III clinical trials for MS.

Materials and Methods

All materials, unless otherwise specified, were purchased from Sigma Aldrich (St. Louis, MO). All procedures involving animals were performed in accordance with standards established in the Guide for the Care and Use of Laboratory Animals as adopted by the U.S. National Institutes of Health. All animal protocols were approved by the Biogen Idec Inc. Institutional Animal Care and Use Committee, which is accredited by the Association for Assessment and Accreditation of Laboratory Animal Care International.

Animal Handling and Tissue RNA Extraction. Wild-type C57BL/6 mice and $Nrf2^{-/-}$ (Itoh et al., 1997) were dosed with a suspension of 0, 50 or 200 mg/kg DMF in 0.8% hydroxypropyl methyl cellulose vehicle (Sigma Aldrich). Drug was delivered by oral gavage at 10 μ L/gram. Tissues were removed 4 hours after dosing and snap frozen in liquid nitrogen then stored at -80°C until use. RNA was prepared from frozen tissues according to manufacturer protocol (RNeasy 96 Universal Tissue Protocol, QIAgen, Hilden Germany). Briefly, frozen tissues were placed in 2 mL 96-well blocks plates with QIAzol (QIAgen) and a 3.2 mm stainless steel bead (BioSpec Products, Bartlesville, OK). Tissues were disrupted for four cycles of 45 seconds in a Mini-Beadbeater (Biospec Products). RNA was extracted in chloroform and the aqueous phase was mixed with 70% ethanol. Extracted RNA was applied to RNeasy96 plates (QIAgen) and purified by the spin method.

Gene Expression Profiling and Quantitative PCR (qPCR). RNA was analyzed for purity and integrity by capillary electrophoresis on Agilent Bioanalyzer 2100 (Agilent Technologies, Santa Clara, CA). Global transcript profiling was done using the Affymetrix GeneChip Mouse 430A 2.0 array (Affymetrix, Santa Clara, CA). Hybridization probe synthesis, microarray hybridization, and scanning were performed according to manufacturer's protocols. Probeset level data were normalized using the robust microarray average algorithm and analyzed with GeneSpring 7.3 data mining software (Agilent Technologies). qPCR was performed from total mRNA isolated from tissues, or from cells extracted using an RNeasy® kit (Qiagen) and reverse-transcribed into cDNA according to manufacturer protocols (Applied Biosystems, Carlsbad, CA). Target gene primers (mouse nicotinamide adenine dinucleotide phosphate dehydrogenase [quinone 1] (NQO1): Mm00500821_m1; mouse aldo-keto reductase family 1, member B8 (AKR1B8): Mm00484314_m1, human heme-oxygenase 1 (HO1): Hs01110250_m1; human Nrf2: Hs00232352_m1; human NQO1: Hs00168547_m1; glutamate-cysteine ligase catalytic subunit (GCLC): Hs00155249_m1) and 6-FAM™ dye-labeled TaqMan® MGB™ probes (Applied Biosystems) were used for qPCR. Reactions containing 100 ng of cDNA, 900 nM of each primer, and 250-nM TaqMan® probes were cycled on a Stratagene Mx3005P™ (Agilent Technologies) once for 10 minutes at 95°C, followed by 40 cycles of 95°C for 10 seconds and 60°C for 1 minute. All samples were measured in duplicate using glyceraldehyde 3-phosphate dehydrogenase as a normalizing gene. Final analysis was performed using the comparative CT

method to calculate fold changes. Samples were normalized relative to vehicle or dimethyl sulfoxide (DMSO) control conditions within each data set.

Cell Culture. Primary cultures of human spinal cord astrocytes, human oligodendrocyte precursor cells (hOPC), human hippocampal neurons (hNeur), and appropriate growth media were purchased from ScienCell Research Laboratories (San Diego, CA) and maintained using supplier specifications. Cells for plate-based assays were seeded into clear bottom tissue culture 24- or 96-well plates (Corning, Lowell, MA). Primary cultures of rat cortical neurons and rat oligodendrocyte precursor cells (rOPCs) were prepared and maintained as previously described (Mi et al., 2009) except for use of the gentleMACS™ system (Miltenyi Biotec, Bergisch Gladbach, Germany) for dissociation.

Compound Handling. DMF and MMF were prepared as 10 mM solutions in DMSO, titrated in DMSO, and then diluted into normal growth media for cell treatments. Final concentration of DMSO (0.3%) was consistent for all treated cells. Following DMF or MMF treatment, cells for use in all assays were washed with Hank's balanced salt solution + 20 mM HEPES, pH 7.4.

Cellular Extract Preparation, Nrf2 Activity Assay, and Western Blotting.

Cytosolic and nuclear extracts were prepared using a nuclear extract kit from Active Motif (Carlsbad, CA). Whole-cell extracts for Western blotting were prepared in 150 mM NaCl, 1.0% Igepal® CA-630, 0.5% sodium deoxycholate, 0.1% SDS, and 50 mM Tris, pH 8.0. Antibodies for Western blotting and the TransAM Nrf2 assay (Active Motif) were used according to manufacturer

instructions. The following antibodies and their suppliers were utilized: Nrf2 (Epitomics, Burlingame, CA or Santa Cruz Biotechnology, Santa Cruz, CA), NQO1 (Epitomics), HO-1 (Epitomics), GCLC (Proteintech Group, Chicago, IL) and actin (MP Biomedical, Solon, OH).

Immunostaining. Immunostaining was performed on cells fixed in 4% paraformaldehyde as previously described (Mi et al., 2009). To increase visualization of nuclear Nrf2 immunostaining, astrocytes were also incubated for 10 minutes with 0.1% SDS in Tris-buffered saline. Primary (Nrf2, Epitomics; β III-tubulin, Millipore, Billerica, MA; glial fibrillary acidic protein, Sigma Aldrich) and secondary (Alexa Fluor 488–labeled, Invitrogen) antibodies were used according to manufacturer instructions. Nuclei were labeled with 4',6 diamidino-2-phenylindole (DAPI) or Hoechst dye, which was included with the secondary antibody incubation. Cells were imaged on a Zeiss Observer Z1 microscope utilizing a 20x LD Plan Neofluar® objective (Carl Zeiss MicroImaging, Thornwood, NY). Astrocyte Nrf2 immunostaining was quantified by random selection and imaging of 10 fields for each condition and captured using identical gain, offset, and accumulation time. Nuclear immunostaining intensity for all nuclei in each field was quantitated in AxioVision (Carl Zeiss MicroImaging). For quantitation of cortical neurons, cells grown in 24-well plates were imaged and counted on the Cellomics ArrayScan® VTi (Thermo Scientific, Pittsburgh, PA) utilizing a neuronal counting protocol to identify intact neurons. Five fields per condition were counted.

Plate-Based Cellular Assays. CellTiter-Blue[®] (Promega, Madison, WI), fluorescent glutathione (GSH) (Sigma Aldrich), LIVE/DEAD[®] (Invitrogen), and ATPLite[™] (PerkinElmer, Waltham, MA) assays were performed according to manufacturer instructions. In general, human astrocytes were plated into 96-well plates, incubated for 4 hours at 37°C, 5% CO₂, then had added DMSO or titrations of DMF or MMF, then incubated for an additional for 20 hours at 37°C, 5% CO₂. For CellTiter-Blue[®], fluorescent GSH, mitochondrial membrane potential and ATP assays, cells were washed with Hank's balanced salt solution + 20 mM HEPES pH 7.4, then incubated with kit reagents as directed. For oxidative challenge experiments, after 20-hour compound incubation, cells were washed and then challenged with 0, 50, or 100 μ M H₂O₂ for 2 hours at 37°C, and then allowed to recover in normal growth media for an additional 20 hours at 37°C, 5% CO₂. Cellular viability was assessed using a LIVE/DEAD[®] viability stain quantified by fluorescence intensity from calcein AM fluorescence in live cells (excitation wavelength: 488 nM, emission wavelength: 525 nM), and also assessed in parallel by counting Hoechst-labeled nuclei using automated imaging and counting. In both assay formats, a subset of DMSO-treated control cells were treated with 0.1% saponin 10 minutes prior to labeling or fixation to generate negative controls on the plate. In the LIVE/DEAD[®] assay, dead cells were labeled with ethidium homodimer and appear red in fluorescent micrographs (excitation wavelength: 550 nM, emission wavelength 575 nM). Live images from LIVE/DEAD[®]-labeled cells were imaged as above. Cell nuclei from Hoechst dye-labeled cells were quantitated in an automated fashion on the Cellomics

ArrayScan VTi platform (Thermo Scientific). Mitochondrial membrane potential was assessed through a ratiometric approach incubating astrocytes with MMF for 20 hours as above, followed by incubation with 100 nM tetramethyl rhodamine ester (TMRE) and 200 nM MitoFluor™ Green (Invitrogen) for 30 minutes at room temperature. The accumulation of TMRE in mitochondria is based on the membrane potential driving intraorganelle accumulation of the anionic probe (Farkas et al., 1989). MitoFluor™ Green was included as a control for total mitochondrial content and to normalize TMRE levels. Signal intensities in the green (excitation wavelength: 488 nm; emission wavelength: 525 nm) and red (excitation wavelength: 550 nm; emission wavelength: 575 nm) channels were measured. Assays were quantitated on EnVision® (PerkinElmer) or FlexStation® (Molecular Devices, Sunnyvale, CA) plate readers. Intracellular calcium levels were measured in astrocytes that were preincubated with a titration of MMF for 20 hours as described, washed, then loaded with a calcium-sensitive dye (Calcium 4; Molecular Devices). Baseline fluorescence values were detected using a FLIPR TETRA® system (Molecular Devices), then H₂O₂ was added to all wells simultaneously to achieve a final concentration of 50 µM, and fluorescence intensities were recorded for a total of 120 minutes. Relative fluorescence units (RFUs) were graphed against time, and the net change in fluorescence over baseline (ΔRFU) was calculated by subtracting the maximum value from the minimum value over the entire recording period.

Small Interfering RNA (siRNA) Analysis. Human spinal cord astrocytes were transfected using the Lonza (Basel, Switzerland) Amaxa T-020 nucleofaction

protocol and the Primary Neurons Solution Kit (Lonza). Cells were transfected with 200 nM Nrf2 specific siRNA (Dharmacon, Dharmacon siGenome duplex D-003755-02-0050) or nonspecific siRNA (Dharmacon, siControl non-targeting siRNA #1). Cells were incubated for 18 to 24 hours after transfection, then treated with a titration of MMF and analyzed in viability assays as described.

Results

DMF-Induced Antioxidant Response in the CNS is Nrf2-Dependent. Previous studies have demonstrated that fumaric acid esters such as DMF and MMF can activate genes typically associated with the Nrf2 antioxidant response pathway (Thiessen et al., 2010; Linker et al., 2011). To ascertain the necessity of Nrf2 in this activation, the global transcriptional response of genes modulated by DMF were examined in both wild-type and Nrf2^{-/-} mice. As is demonstrated here in the spleen, wild-type mice responded to DMF with a significant upregulation of 738 genes compared with only 7 transcripts in Nrf2^{-/-} mice (changes with $p < 10^{-5}$; Fig. 1A). Analysis of Akr1b8 expression, a known Nrf2 target gene, provided further evidence that Nrf2 was essential for DMF-induced antioxidant response in the spleen (Fig. 1B). The transcriptional changes in response to DMF treatment were somewhat tissue-type specific. In colon, both NQO1 and Akr1b8 were upregulated, whereas in other tissues such as liver and duodenum, Akr1b8 was significantly upregulated while NQO1 exhibited modest to no induction, and mesenteric lymph nodes exhibited an opposite pattern of increased NQO1 and

little change in Akr1b8 (Supplemental Fig. 1). In brain, NQO1 message levels were significantly increased also in an Nrf2 dependent fashion (Fig. 1C).

Fumarates Activate the Nrf2 Pathway in CNS Cells. Recent studies have described a potential neuroprotective mechanism of action for DMF and MMF demonstrated from in vitro and in vivo data (Ellrichmann et al., 2011; Linker et al., 2011). To discern direct molecular events around this mechanism, primary cultures of spinal cord astrocytes were exposed to DMF or MMF for 6 hours and assessed for Nrf2 expression using immunofluorescent microscopy (Fig. 2A). Mean nuclear densitometric immunostaining intensity was increased relative to DMSO controls, by 63.9% with DMF and 37.5% with MMF (Fig. 2B). Nrf2 activity in these cells was mostly confined to the nuclear fraction and was 2- to 5-fold greater than seen with DMSO controls, as determined by both Nrf2 DNA binding assays and Western immunoblots (Fig. 2C). The fidelity of the nuclear and cytoplasmic preparations was confirmed by Western immunoblots for nuclear-specific protein (HDAC; Fig. 2C). Immunoblotting for Nrf2 in hOPCs and rOPCs, as well as hNeur treated with 10 μ M DMF or MMF, confirmed that all CNS cell types showed increased Nrf2 levels over time (Fig. 2D). In several of the cell types a doublet of Nrf2 immunoreactivity was observed on Western immunoblots, with only the upper band exhibiting sensitivity to modulation by DMF or MMF and enrichment in nuclear fractions (Fig. 2C, D). Replicate immunoblots for these cell types were probed with NQO1 antibody to examine a prototypical Nrf2 target gene and showed that after 24 hours there was a robust increase in NQO1 in hOPCs with DMF and MMF treatment, but this increase was only obvious with

DMF in rOPCs. Human neurons or rOPCs treated with MMF had a milder response, with relatively minor increases at 24 hours (Fig. 2D).

Previous work from our laboratory and others have demonstrated that fumarates can activate downstream transcription of a number of canonical Nrf2 target genes, however the majority of these studies have been performed in cultured cells lines or assessed in non-CNS tissues (Linker et al., 2011). Activation of the Nrf2 transcriptional pathway by DMF and MMF was confirmed from analysis of Nrf2 mRNA levels in primary astrocyte cultures. A modest, but significant, approximately 2-fold transient increase in Nrf2 mRNA was observed following 2 and 4 hours of DMF treatment, but no changes were observed with MMF treatment, although robust stabilization of the Nrf2 protein was observed (Fig. 3A). There was a greater accumulation of Nrf2 with DMF treatment, however the levels of Nrf2 appeared more consistent at the later 24 hour time point with MMF treatment (Fig. 3A). The expression profiles of several canonical Nrf2-responsive genes were also probed at the mRNA and protein level. NQO1 (Fig. 3B), HO1 (Fig. 3C) and GCLC (Fig. 3D) all demonstrated significant induction by MMF or DMF, although the temporal aspect varied between analytes. NQO1 appeared to gradually accumulate mRNA and protein over time (Fig. 3B), whereas in contrast GCLC exhibited a transient induction in mRNA between 4 and 6 hours that translated into increased protein from 6 to 24 hours, by which time message levels had returned to baseline (Fig. 3D). HO1 also demonstrated a fairly transient response with mRNA and protein levels peaking from 4 to 6 hours then declining out to 24 hours (Fig. 3C). While not a

comprehensive profile of Nrf2-responsive genes, these data suggest that human astrocytes are capable of responding to MMF and DMF treatment leading to induction of a prototypical phase II antioxidant response.

MMF Treatment Increases Cellular Redox Potential. To further explore the molecular changes induced by DMF and MMF treatment, primary cultures of human astrocytes were used to assess functional consequences of stimulating the Nrf2 pathway. These, and most subsequent experiments, describe the use of MMF, as although DMF appeared more potent in inducing the Nrf2 response in vitro (Fig. 3A), preclinical animal and human clinical data have demonstrated that DMF is quantitatively converted to MMF very rapidly after oral dosing (Biogen Idec, data not shown). This indicates systemically, cells and tissues are only exposed to MMF after an oral DMF dose, making MMF the more relevant fumarate species for in vitro use. Following overnight treatment with MMF, astrocytes were incubated with resazurin, an oxidized substrate that changes fluorescent properties when reduced to resorufin by metabolically active cells. This should thus provide a relative assessment of cellular redox potential based on ability to reduce oxidized substrates, since the substrate was supplied in excess. Increasing concentrations of MMF significantly increased the levels of resorufin, with a maximal 35% increase over baseline at 30 μ M MMF (Fig. 4A). GSH, a primary cellular biomolecule for detoxifying free radicals, was dose-dependently increased by MMF (maximal increase 18% at 30 μ M) when treated cells were incubated with the thiol-containing molecule monochlorobimane (Fig. 4B). MMF also appeared to promote modest, but significant increases

(approximately 5%) in cellular ATP content, relative to DMSO controls (Fig. 4C). These increases in ATP levels may be due to enhanced production of ATP, as would be expected to occur in response to changes in the mitochondrial membrane potential, which drives the electron transport chain and ATP biosynthesis. Supporting this hypothesis, MMF-treatment significantly increased the mitochondrial membrane potential in a concentration-dependent fashion, as shown by increased TMRE: MitoFluor™ Green ratios (maximal increase 2.3-fold at 10 and 30 μ M, Fig. 4D). TMRE accumulates in the mitochondria based on the membrane potential of this organelle driving accumulation of the anionic probe. Taken together, these data suggest DMF and MMF treatment “primes” cells and increases their capacity for dealing with oxidative stress by increasing the intrinsic pathways that result in enhanced biosynthesis of detoxification molecules such as glutathione.

DMF and MMF Enhance Viability After Oxidative Stress. To begin characterizing the functional effects of DMF and MMF treatment, primary cultures of human astrocytes were subjected to oxidative stress using H_2O_2 and assessed for changes in intracellular calcium accumulation. Changes in these levels were assessed using Calcium 4 dye fluorescence recorded over a 120-minute period in cells treated with a titration of MMF, then challenged with H_2O_2 (Fig. 5A). DMSO control cells challenged with H_2O_2 showed an approximate 50% increase in calcium over unchallenged controls, whereas increasing concentrations of MMF progressively reduced H_2O_2 -induced increases back to baseline levels (Fig. 5B).

As abnormal intracellular calcium accumulation is known to trigger apoptotic cascades and destabilize mitochondrial energy metabolism, the effects of DMF and MMF treatment and H₂O₂ challenge on cellular viability was assessed. To identify potential confounding effects of DMF and MMF cytotoxicity, both compounds were assessed and in both LIVE/DEAD[®] and nuclei counting assays under conditions of no oxidative stress (0 μM H₂O₂). These results suggested that in these cells, DMF was cytotoxic at concentrations of 33 μM and 100 μM (Fig. 5C, E green bars), whereas MMF treatment (Fig. 5D, F, green bars) resulted in less toxicity (only at 100 μM). Addition of 50 μM H₂O₂ to DMSO treated cells in the absence of DMF or MMF resulted in approximately 66% reductions in fluorescence intensity in the LIVE/DEAD[®] assay and 75% reductions in nuclei counts (Fig. 5C-F). Non-toxic concentrations of DMF (Fig. 5C, E) and MMF (Fig. 5D, F) improved cellular viability in both assay formats. Consistent with Nrf2 pathway activation data (Fig. 2B-D, 3A-D), DMF appeared to be more potent than MMF in protecting astrocytes from oxidative challenge; however the maximal protective response was similar for both compounds (Fig. 5C-F). The cytoprotective effects conferred by DMF or MMF treatment were overcome by 100 μM H₂O₂ challenge, at which only minor trends in protection were observed (Figure 5C-F). To confirm the fluorescence intensity-based quantitative results (Fig. 5C-F), imaging assessments from samples used in the LIVE/DEAD[®] assay were performed. Saponin-treated negative controls (Fig. 5G) clearly showed a lack of live cells whereas DMSO positive controls showed a uniform confluent layer of viable cells (Fig. 5H). Challenging the DMSO-treated

cells with 50 μM H_2O_2 resulted in a dramatic increase in dead cells and a change in morphology of the viable cells to a more rounded structure that is characteristic of cells undergoing apoptotic or other toxicity-related death (Fig. 5I).

Pretreatment of the astrocytes with MMF resulted in preservation of viability and morphology (Fig. 5J). However, MMF did not prevent loss of all cells as can be seen from the decreased density of viable cells (Fig. 5J compared to Fig. 5H). These data, using multiple different types of assay formats, suggested that both DMF and MMF were able to promote cytoprotective responses in cells such that they were better able to withstand oxidative stress, and thus had improved viability after a toxic challenge.

To extend these data and determine if the direct cytoprotective responses of DMF and MMF were consistent in other CNS cell types, cortical cultures from embryonic rat pups were utilized in a similar H_2O_2 challenge paradigm. Fixed cultures were immunostained for the neuronal marker protein β III-tubulin and nuclei were labeled with DAPI. Control cultures showed healthy neural cells, with all neurons extending both highly branched and unbranched neurites (Fig. 6A). Challenging with 10 μM H_2O_2 caused an 80% loss in neurons (Fig. 6B, D). However, cells that were pretreated with MMF exhibited significant protection from the oxidative insult with a maximal 55% increase in viability at 10 μM MMF (Fig. 6C, D). These data confirmed that MMF can act on multiple CNS-resident cell types and confer cytoprotective responses against oxidative stress.

MMF-Induced Cytoprotection Is Nrf2-Dependent. The role of Nrf2 in mediating DMF or MMF-dependent cytoprotection was assessed by reducing Nrf2 mRNA

and protein using Nrf2-specific siRNA. Transfection of human astrocytes with control siRNA resulted in a small decrease in Nrf2 levels following induction with 10 μ M DMF (Fig. 7A, B). In contrast, cultures transfected with Nrf2 siRNA had lower basal levels of Nrf2, and did not appear to have increased Nrf2 protein after DMF treatment (Fig. 7A, B). These data indicated that the Nrf2 siRNA was capable of reducing total Nrf2 protein and prevented the DMF-dependent increase in Nrf2. To determine the effects of reducing Nrf2 protein, astrocytes were transfected with either control or Nrf2 siRNA, then treated with DMSO as a control or a titration of MMF for 20 hours, then subjected to 50 μ M H₂O₂ challenge. This analysis demonstrated that in control siRNA conditions, MMF was able to confer cytoprotective responses on H₂O₂ challenged astrocytes in a concentration-dependent fashion (Fig. 7C), similar to previous data in untransfected cells (Fig. 5D, J). However, in cells transfected with Nrf2 siRNA, and challenged with 50 μ M H₂O₂, MMF had no cytoprotective effects at any concentration tested (Fig. 7C), suggesting Nrf2 protein was required for MMF-dependent cytoprotection against oxidative stress.

Discussion

Many studies have indicated that targeting the Nrf2 pathway presents a potentially potent mechanism to combat the oxidative stress associated with several different neurodegenerative diseases (Calkins et al., 2009). Targeting the Nrf2 pathway with small molecule activators presents an attractive opportunity

since the target is an intrinsic cellular pathway that is designed to be dynamically modulated. The need for this type of therapy in MS is clear, as current evidence indicates free radicals play a large role in MS pathogenesis (van Horssen et al., 2010), with damage to protein, lipid and DNA in the tissues and cells proximal to lesion areas and in circulation (Vladimirova et al., 1998; Ferretti et al., 2005; van Horssen et al., 2008). Interestingly, these studies have shown that some antioxidant response proteins, including Nrf2, are elevated in MS lesions (van Horssen et al., 2008; van Horssen et al., 2010), however the degree of intrinsic antioxidant induction is apparently insufficient to ultimately prevent disease progression. Our observations have shown that DMF and MMF can activate the Nrf2 pathway in multiple CNS-resident cell types both in vitro and in vivo, stabilizing levels of Nrf2 protein, resulting in the accumulation of active transcription factor and translocation into the nucleus, thereby conferring cytoprotective responses against oxidative stress. Profiling of known Nrf2 target genes, such as NQO1, suggests that astrocytes, OPCs and perhaps neurons are capable of responding to MMF and DMF treatment, leading to induction of a prototypical Nrf2-dependent antioxidant response. Detailed profiling is currently underway to characterize CNS cell-type and brain region specific transcriptional responses to DMF and MMF treatment.

In addition to characterization of Nrf2 pathway activation in CNS cells, a potential downstream functional mechanism by which DMF or MMF may promote resistance to oxidative stress has been identified. The studies described here demonstrated that MMF treatment can increase cellular GSH levels in astrocytes

(Fig. 4B) consistent with the demonstrated upregulation of GCLC (Fig. 3D), a rate-limiting enzyme in GSH biosynthesis. GSH is the main cellular antioxidant against ROS, thus increased levels of this thiol-containing tripeptide would promote increased ability to detoxify and survive oxidative stress. The MMF-dependent increases observed at 20 hours after treatment are not necessarily inconsistent with previous findings, which demonstrated no acute changes to GSH levels over 60 minutes of MMF treatment (Schmidt and Dringen 2010; Thiessen et al., 2010). The protein profiling analysis demonstrated that at least some enzymatic components involved in GSH biosynthesis, such as GCLC, were not upregulated until several hours after treatment (Fig. 3D), indicating that 60 minutes may be an insufficient time in order to observe these changes. Recent *in vivo* evidence also supports a role for activation of the Nrf2 pathway in increasing CNS GSH levels. These data suggested that enhanced astrocyte GSH biosynthesis and secretion lead to increased extracellular cysteine as a product of GSH metabolism, which was then transported into neurons via upregulation of the excitatory amino acid transporter 3, and ultimately drove increased neuronal GSH due to increased levels of biosynthetic substrate (Escartin et al., 2011). Elucidation of this pathway suggests a potential role for cell-type specific neuroprotective responses, and is consistent with the astrocyte data presented here. It is clear that increasing cellular GSH levels in the CNS could have a meaningful therapeutic impact in MS, as reduced brain GSH levels have been reported in MS patients, as measured using magnetic resonance spectroscopy (Choi et al., 2010; Srinivasan et al., 2010). Therapies in clinical trials for MS,

such as BG-12, which is an oral therapeutic containing DMF as the active ingredient (which is quantitatively converted to MMF after oral DMF delivery), could increase cellular GSH levels (Fig. 4B) and may offer an opportunity to restore redox balance in the CNS of patients. This could have a meaningful therapeutic impact by potentially offering greater protection against the neurodegenerative effects of disease-related increases in oxidative stress.

Mitochondrial dysfunction may also play a major role in the pathogenesis of neurodegenerative diseases, particularly in MS, where reduced mitochondrial function in the CNS has been observed (Dutta et al., 2006; Mahad et al., 2009), despite increased mitochondrial content (Blokhin et al., 2008; Witte et al., 2009). This seemingly paradoxical situation possibly reflects a compensatory mechanism for reduced energy output from individual mitochondrion. Our data obtained in astrocytes may indicate that MMF could potentially alleviate some of this mitochondrial dysfunction, as modest, but significant, increases in cellular ATP content (Fig. 4C) and mitochondrial membrane polarization (Fig. 4D) were observed following treatment. It is also important to note that mitochondria have a critical role in buffering intracellular calcium, and interestingly, MMF was able to prevent the H₂O₂-induced abnormal accumulation of intracellular calcium (Fig. 5A, B). However, it was not clear if this was due to improved mitochondrial buffering capacity via enhancement of the electrochemical gradient and subsequent increased calcium ionic flux, or due to direct detoxification of the oxidative challenge via MMF-induced Nrf2 antioxidant response. The mechanism

by which MMF may increase mitochondrial energy metabolism and membrane potential remains unclear.

Our results, using multiple types of assay formats, indicate that both DMF and MMF are able to promote cytoprotective responses in cells by activating the Nrf2 pathway, enabling them to better withstand oxidative stress. The attenuation of H₂O₂-induced calcium accumulation, along with potential mitigation of other cellular events related to toxic oxidative challenge ultimately resulted in MMF or DMF-dependent increase in viability in astrocytes and neurons. Nrf2 appeared to be required for these effects. The oxidative injury and challenge paradigms explored here are highly relevant to the mechanistic damage that occurs in MS, and collectively these preclinical studies using DMF and its primary metabolite MMF provide a compelling rationale for the use of BG-12 as a therapeutic agent in the treatment of MS.

Acknowledgments

The authors would like to thank Mark Hughes, Simon Whiteley and Heather Sun for reviewing this manuscript and for providing editing assistance.

Authorship Contributions

Participated in research design: Scannevin, Chollate, Jung, Shackett, Patel, Ryan, Lukashev, Rhodes

Conducted experiments: Scannevin, Chollate, Jung, Shackett, Patel, Bista, Zeng, Ryan

Contributed new reagents or analytic tools: Scannevin, Bista, Zeng, Ryan, Yamamoto

Performed data analysis: Scannevin, Chollate, Jung, Shackett, Patel, Bista, Zeng, Ryan, Lukashev

Wrote or contributed to the writing of the manuscript: Scannevin, Ryan, Lukashev, Rhodes

References

- Blokhin A, Vyshkina T, Komoly S, and Kalman B (2008) Variations in mitochondrial DNA copy numbers in MS brains. *J Mol Neurosci* **35**(3): 283-287.
- Calabrese V, Colombrita C, Guagliano E, Sapienza M, Ravagna A, Cardile V, Scapagnini G, Santoro AM, Mangiameli A, Butterfield DA, Giuffrida Stella AM, and Rizzarelli E (2005) Protective effect of carnosine during nitrosative stress in astroglial cell cultures. *Neurochem Res* **30**(6-7): 797-807.
- Calkins MJ, Johnson DA, Townsend JA, Vargas MR, Dowell JA, Williamson TP, Kraft AD, Lee JM, Li J, and Johnson JA (2009) The Nrf2/ARE pathway as a potential therapeutic target in neurodegenerative disease. *Antioxid Redox Signal* **11**(3): 497-508.
- Cao X, Xiao H, Zhang Y, Zou L, Chu Y, and Chu X (2010) 1, 5-Dicaffeoylquinic acid-mediated glutathione synthesis through activation of Nrf2 protects against OGD/reperfusion-induced oxidative stress in astrocytes. *Brain Res* **1347**: 142-148.
- Chen PC, Vargas MR, Pani AK, Smeyne RJ, Johnson DA, Kan YW, and Johnson JA. (2009) Nrf2-mediated neuroprotection in the MPTP mouse model of Parkinson's disease: Critical role for the astrocyte. *Proc Natl Acad Sci U S A* **106**(8): 2933-2938.

Choi IY, Lee SP, Denney DR, and Lynch SG (2010) Lower levels of glutathione in the brains of secondary progressive multiple sclerosis patients measured by ¹H magnetic resonance chemical shift imaging at 3 T. *Mult Scler* **17**(3): 289-296.

Dumont M, Wille E, Calingasan NY, Tampellini D, Williams C, Gouras GK, Liby K, Sporn M, Nathan C, Flint Beal M, and Lin MT (2009) Triterpenoid CDDO-methylamide improves memory and decreases amyloid plaques in a transgenic mouse model of Alzheimer's disease. *J Neurochem* **109**(2): 502-512.

Dutta R, McDonough J, Yin X, Peterson J, Chang A, Torres T, Gudz T, Macklin WB, Lewis DA, Fox RJ, Rudick R, Mirnics K, and Trapp BD (2006) Mitochondrial dysfunction as a cause of axonal degeneration in multiple sclerosis patients. *Ann Neurol* **59**(3): 478-489.

Ellrichmann G, Petrasch-Parwez E, Lee DH, Reick C, Arning L, Saft C, Gold R, and Linker RA (2011) Efficacy of fumaric acid esters in the R6/2 and YAC128 models of Huntington's disease. *PLoS One* **6**(1): e16172.

Escartin C, Won SJ, Malgorn C, Auregan G, Berman AE, Chen PC, Déglon N, Johnson JA, Suh SW, and Swanson RA (2011) Nuclear factor erythroid 2-related factor 2 facilitates neuronal glutathione synthesis by upregulating neuronal excitatory amino Acid transporter 3 expression. *J Neurosci* **31**(20): 7392-7401.

Farkas DL, Wei MD, Febroriello P, Carson JH, and Loew LM (1989)

Simultaneous imaging of cell and mitochondrial membrane potentials. *Biophys J* **56**(6): 1053-1069.

Ferretti G, Bacchetti T, Principi F, Di Ludovico F, Viti B, Angeleri VA, Danni M, and Provinciali L (2005) Increased levels of lipid hydroperoxides in plasma of patients with multiple sclerosis: a relationship with paraoxonase activity. *Mult Scler* **11**(6): 677-682.

Hardingham G E and Lipton SA (2010) Regulation of neuronal oxidative and nitrosative stress by endogenous protective pathways and disease processes. *Antioxid Redox Signal* **14**(8): 1421-1424.

Itoh K, Chiba T, Takahashi S, Ishii T, Igarashi K, Katoh Y, Oyake T, Hayashi N, Satoh K, Hatayama I, Yamamoto M, and Nabeshima Y (1997) An Nrf2/small Maf heterodimer mediates the induction of phase II detoxifying enzyme genes through antioxidant response elements. *Biochem Biophys Res Commun* **236**(2): 313-322.

Itoh K, Tong KI, and Yamamoto M (2004) Molecular mechanism activating Nrf2-Keap1 pathway in regulation of adaptive response to electrophiles. *Free Radic Biol Med* **36**(10): 1208-1213.

Jakel RJ, Townsend JA, Kraft AD, and Johnson JA (2007) Nrf2-mediated protection against 6-hydroxydopamine. *Brain Res* **1144**: 192-201.

Kwak MK, Wakabayashi N, Itoh K, Motohashi H, Yamamoto M, and Kensler TW (2003) Modulation of gene expression by cancer chemopreventive dithiolethiones through the Keap1-Nrf2 pathway. Identification of novel gene clusters for cell survival. *J Biol Chem* **278**(10): 8135-8145.

Lee JM, Calkins MJ, Chan K, Kan YW, and Johnson JA (2003) Identification of the NF-E2-related factor-2-dependent genes conferring protection against oxidative stress in primary cortical astrocytes using oligonucleotide microarray analysis. *J Biol Chem* **278**(14): 12029-12038.

Li J, Johnson D, Calkins M, Wright L, Svendsen C, and Johnson J (2005) Stabilization of Nrf2 by tBHQ confers protection against oxidative stress-induced cell death in human neural stem cells. *Toxicol Sci* **83**(2): 313-328.

Li W and Kong AN (2009) Molecular mechanisms of Nrf2-mediated antioxidant response. *Mol Carcinog* **48**(2): 91-104.

Lin SX, Lisi L, Russo CD, Polak PE, Sharp A, Weinberg G, Kalinin S, and Feinstein DL (2011) The anti-inflammatory effects of dimethyl fumarate in astrocytes involve glutathione and heme-oxygenase 1. *ASN Neuro* **3**(2): e00055.

Linker RA, Lee DH, Ryan S, van Dam AM, Conrad R, Bista P, Zeng W, Hronowsky X, Buko A, Chollate S, Ellrichmann G, Brück W, Dawson K, Goelz S, Wiese S, Scannevin RH, Lukashev M, and Gold R (2011) Fumaric acid esters exert neuroprotective effects in neuroinflammation via activation of the Nrf2 antioxidant pathway. *Brain* **134**(3): 678-692.

Mahad DJ, Ziabreva I, Campbell G, Lax N, White K, Hanson PS, Lassmann H, and Turnbull DM (2009) Mitochondrial changes within axons in multiple sclerosis. *Brain* **132**(5): 1161-1174.

Mi S, Miller RH, Tang W, Lee X, Hu B, Wu W, Zhang Y, Shields CB, Zhang Y, Miklasz S, Shea D, Mason J, Franklin RJ, Ji B, Shao Z, Chédotal A, Bernard F, Roulois A, Xu J, Jung V, and Pepinsky B (2009) Promotion of central nervous system remyelination by induced differentiation of oligodendrocyte precursor cells. *Ann Neurol* **65**(3): 304-315.

Neymotin A, Calingasan NY, Wille E, Naseri N, Petri S, Damiano M, Liby KT, Risingsong R, Sporn M, Beal MF, and Kiaei M (2011) Neuroprotective effect of

Nrf2/ARE activators, CDDO ethylamide and CDDO trifluoroethylamide, in a mouse model of amyotrophic lateral sclerosis. *Free Radic Biol Med* **51**(1):88-96.

Nguyen T, Sherratt PJ, and Pickett CB (2003) Regulatory mechanisms controlling gene expression mediated by the antioxidant response element. *Annu Rev Pharmacol Toxicol* **43**: 233-260.

Schilling S, Goelz S, Linker R, Luehder F, and Gold R (2006) Fumaric acid esters are effective in chronic experimental autoimmune encephalomyelitis and suppress macrophage infiltration. *Clin Exp Immunol* **145**(1): 101-107.

Schmidt MM and Dringen R (2010) Fumaric acid diesters deprive cultured primary astrocytes rapidly of glutathione. *Neurochem Int* **57**(4): 460-467.

Soane L, Li Dai W, Fiskum G, and Bambrick LL (2010) Sulforaphane protects immature hippocampal neurons against death caused by exposure to hemin or to oxygen and glucose deprivation. *J Neurosci Res* **88**(6): 1355-1363.

Srinivasan R, Ratiney H, Hammond-Rosenbluth KE, Pelletier D, and Nelson SJ (2010) MR spectroscopic imaging of glutathione in the white and gray matter at 7 T with an application to multiple sclerosis. *Magn Reson Imaging* **28**(2): 163-170.

Stack C, Ho D, Wille E, Calingasan NY, Williams C, Liby K, Sporn M, Dumont M, and Beal MF (2010) Triterpenoids CDDO-ethyl amide and CDDO-trifluoroethyl amide improve the behavioral phenotype and brain pathology in a transgenic mouse model of Huntington's disease. *Free Radic Biol Med* **49**(2): 147-158.

Thiessen AM, Schmidt M and Dringen R (2010) Fumaric acid dialkyl esters deprive cultured rat oligodendroglial cells of glutathione and upregulate the expression of heme oxygenase 1. *Neurosci Lett* **475**(1): 56-60.

Tran TA, McCoy MK, Sporn MB, and Tansey MG (2008) The synthetic triterpenoid CDDO-methyl ester modulates microglial activities, inhibits TNF production, and provides dopaminergic neuroprotection. *J Neuroinflammation* **5**: 14.

van Horssen J, Drexhage JA, Flor T, Gerritsen W, van der Valk P, and de Vries HE (2010) Nrf2 and DJ1 are consistently upregulated in inflammatory multiple sclerosis lesions. *Free Radic Biol Med* **49**(8): 1283-1289.

van Horssen J, Schreibelt G, Drexhage J, Hazes T, Dijkstra CD, van der Valk P, and de Vries HE (2008) Severe oxidative damage in multiple sclerosis lesions coincides with enhanced antioxidant enzyme expression. *Free Radic Biol Med* **45**(12): 1729-1737.

van Horssen J, Witte ME, Schreibelt G, and de Vries HE (2010) Radical changes in multiple sclerosis pathogenesis. *Biochim Biophys Acta* **1812**(2): 141-150.

Vargas MR, Johnson DA, Sirkis DW, Messing A, and Johnson JA (2008) Nrf2 activation in astrocytes protects against neurodegeneration in mouse models of familial amyotrophic lateral sclerosis. *J Neurosci* **28**(50): 13574-13581.

Vladimirova O, O'Connor J, Cahill A, Alder H, Butunoi C, and Kalman B (1998) Oxidative damage to DNA in plaques of MS brains. *Mult Scler* **4**(5): 413-418.

Witte ME, Bø L, Rodenburg RJ, Belien JA, Musters R, Hazes T, Wintjes LT, Smeitink JA, Geurts JJ, De Vries HE, van der Valk P, and van Horssen J (2009) Enhanced number and activity of mitochondria in multiple sclerosis lesions. *J Pathol* **219**(2): 193-204.

Yang L, Calingasan NY, Thomas B, Chaturvedi RK, Kiaei M, Wille EJ, Liby KT, Williams C, Royce D, Risingsong R, Musiek ES, Morrow JD, Sporn M, and Beal MF (2009) Neuroprotective effects of the triterpenoid, CDDO methyl amide, a potent inducer of Nrf2-mediated transcription. *PLoS One* **4**(6): e5757.

Figure Legends

Fig. 1. DMF induction of an antioxidant response in the CNS was Nrf2-dependent. Wild-type (WT) or Nrf2^{-/-} (KO) mice were treated with 0, 50 or 200 mg/kg DMF by oral gavage. Tissues were harvested 4 hours after DMF dosing. **A**, global transcriptional profiling of spleen tissue revealed induction of 738 specific genes with $p < 10^{-5}$ in wild-type mice, whereas in Nrf2^{-/-} mice only 7 transcripts were found to have changed in response to 200 mg/kg DMF treatment. **B**, analysis of spleen tissue using quantitative PCR to characterize expression level differences of Akr1b8 between wild-type (gray bars) and Nrf2^{-/-} (white bars) mice. **C**, similar analysis as in (B) using brain tissue and quantitation of NQO1 transcript levels. ** $p < 0.01$, *** $p < 0.001$, based on two-way ANOVA with Dunnett's post-test for multiple-sample comparison against the relevant WT or KO vehicle group.

Fig. 2. DMF and MMF increased Nrf2 in CNS cells. **A**, human astrocytes were treated with DMSO or 10 μ M DMF or MMF for 6 hours, then fixed, permeabilized, and immunostained for Nrf2. Left panels are images of DMSO-treated samples; the top-right image shows cells treated with DMF and bottom right image shows cells treated with MMF. Presented images have identical histogram lookup tables for display comparison. **B**, mean nuclear immunostaining intensity was quantitated for every cell in 5 fields from each condition. **C**, astrocytes were treated with either DMSO, 3 μ M DMF, 30 μ M DMF, 3 μ M MMF, or 30 μ M MMF for 6 hours. Extracts from harvested cells were separated into nuclear or

cytoplasmic fractions. Equal protein amounts from replicate aliquots of each fraction were tested in an Nrf2 DNA binding assay and Western immunoblots were probed with antibodies for Nrf2 or HDAC. **D**, Nrf2 and NQO1 Western immunoblots of extracts from hOPCs, hNeur and rOPCs were treated with 10 μ M DMF or MMF, then harvested after 1, 2, 4, 6, or 24 hours of treatment. The 0-hour time point represents the DMSO control sample. *** $p < 0.001$ based on one-way ANOVA with Dunnett's multiple comparison post test against DMSO control.

Fig. 3. DMF and MMF induced upregulation of canonical Nrf2 pathway antioxidant genes and proteins. Human astrocytes were treated with DMSO or 10 μ M DMF or MMF, and replicate cultures were harvested at 1, 2, 4, 6, or 24 hours after compound addition. Duplicate cultures were harvested at each time point for RNA extraction and subsequent qPCR and to generate a cell extract for Western immunoblotting. Relative mRNA (bar graphs) and protein levels (Western immunoblots of **A**, Nrf2, **B**, NQO1, **C**, HO1, and **D**, GCLC were assessed. For qPCR data, the average fold change relative to normalized DMSO control was plotted; the error bar represents SD, and $n = 4$ for all assays. * $p < 0.05$ based on one-way ANOVA with Dunnett's post-test for multiple-sample comparison against the DMSO 0-hour time point control.

Fig. 4. MMF treatment enhanced cellular redox potential by increasing glutathione and ATP levels. Human astrocytes were treated with a titration of MMF and then assessed for **A**, cellular redox potential, **B**, glutathione levels, **C**,

total ATP levels, and **D**, mitochondrial membrane potential. (A, B, C) are presented as a percentage relative to DMSO control–treated cells. Mitochondrial membrane potential in (D) is represented as the average ratio of TMRE intensity to MitoFluor Green intensity to normalize for total cellular mitochondrial content. Error bars represent SD; minimum $n = 8$. $*p < 0.05$ based on one-way ANOVA analysis and Dunnett’s multiple comparison post test against DMSO controls.

Fig. 5. DMF and MMF promoted direct cytoprotection after oxidative challenge in astrocytes. The functional effects of MMF treatment were assessed in human astrocytes that were treated with a titration of MMF and then challenged with H_2O_2 . **A**, real-time analysis of intracellular calcium as visualized by Calcium-4 fluorescence (RFU) in treated astrocytes followed for 120 minutes (recording once every minute) after a 50 μM H_2O_2 challenge. Differently colored traces represent different MMF concentrations as indicated. Arrow denotes time of H_2O_2 addition. **B**, quantification of change in RFU based on difference of maximum and minimum signals over recording period. Graph represents average ΔRFU for each indicated condition, error bars represent SD, each condition done in quadruplicate. Red dashed line represents maximal H_2O_2 -induced calcium accumulation; green dashed line represents basal calcium accumulation in the absence of H_2O_2 challenge. **C, D**, Quantification of calcein AM fluorescence intensity (RFU) in LIVE/DEAD®-labeled cells pretreated with a titration of **C**, DMF or **D**, MMF and then challenged with 0, 50, or 100 μM H_2O_2 followed by a 20-hour recovery prior to analysis. **E, F**, Replicate plates as in (C, D) fixed and

stained with Hoechst dye. Graphs represent average cell nuclei counts in 10 fields per condition. **G–J**, live imaging of cells from (C–F); “LIVE” calcein AM (green) and “DEAD” ethidium homodimer (red) labeling. Presented images have identical histogram lookup tables for display comparison. **G**, negative control cells preincubated with 0.1% saponin to permeabilize plasma membranes. **H**, positive control cells treated with DMSO. **I**, control DMSO–treated and 50 μM H_2O_2 –challenged cells. **J**, astrocytes pretreated with 11 μM MMF and challenged with 50 μM H_2O_2 . Error bars represent SD in C–F.

Fig. 6. MMF promotes cytoprotection of rat cortical neurons after oxidative challenge. Representative images and quantitation from **A**, control rat primary cortical neuronal cultures from E18 pups grown for 7 days in vitro; **B**, replicate cortical culture incubated with 10 μM H_2O_2 for 2 hours then recovered for 20 hours; and **C**, replicate cortical culture treated with 0, 3.3, 10, or 30 μM MMF for 20 hours prior to 10 μM H_2O_2 challenge and 20-hour recovery. (A–C) All cultures were immunostained with β III-tubulin (green) and DAPI (blue). Presented images have identical histogram lookup tables for display comparison. **D**, quantification of neuronal counts from 5 fields from each condition. Graph represents the mean percentage of each condition relative to non- H_2O_2 challenged controls. Error bars represent SD. * $p < 0.05$ based on one way ANOVA analysis and Dunnett’s multiple comparison post-test against “0 μM + H_2O_2 ” DMSO controls.

Fig. 7. Astrocyte cytoprotection conferred by MMF was dependent upon Nrf2.

Human astrocytes that were untransfected, or transfected with either control or Nrf2-specific siRNA were analyzed. **A**, replicate control and transfected astrocytes were separated into two different groups: “untreated” cells, which were transfection with indicated siRNA, then harvested 20 hrs after transfection and “DMF 24h” cells, which were transfected, incubated for 20 hours, then treated with 30 μ M DMF, for 20 hours prior to preparation of cellular extracts. Western immunoblots of cell extracts were probed with antibodies to Nrf2 or actin. **B**, quantitation of Western immunoblot in (A). **C**, Astrocyte viability; cells were transfected with control or Nrf2 siRNA, treated with a titration of MMF, and then challenged with 0 μ M H₂O₂ (black bars) or 50 μ M H₂O₂ (gray bars). Valid cell counts were determined in cells that were positive for glial fibrillary acidic protein immunostaining and DAPI staining. The graph represents average cell counts per well in quadruplicate wells; error bars indicate SD.

Tables

Table 1. Structure and Basic Properties of Dimethyl Fumarate (DMF) and Monomethyl Fumarate (MMF)

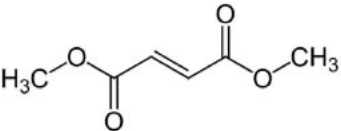
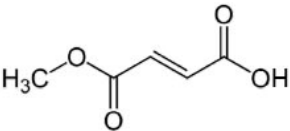
Compound Name	Dimethyl fumarate	Monomethyl fumarate
Abbreviation	DMF	MMF
Structure		
Molecular weight	144.13	130.1
Molecular Formula	C ₆ H ₈ O ₄	C ₅ H ₆ O ₄

Figure 1

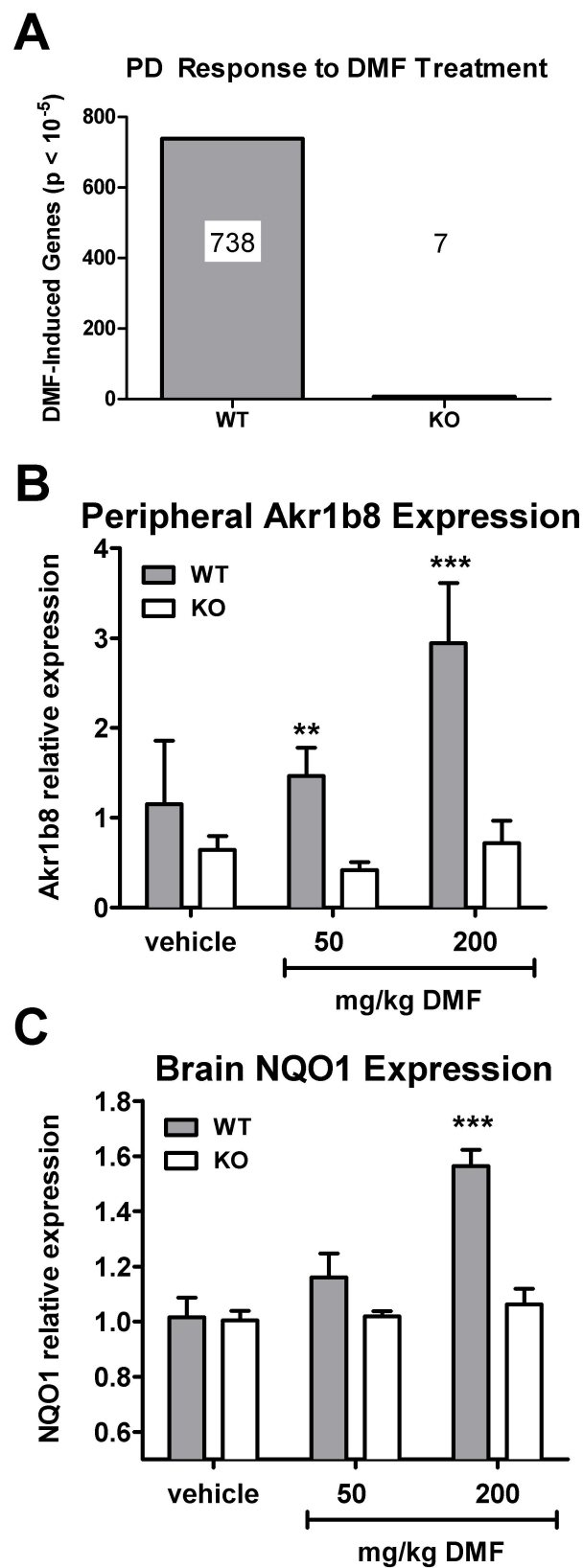


Figure 2

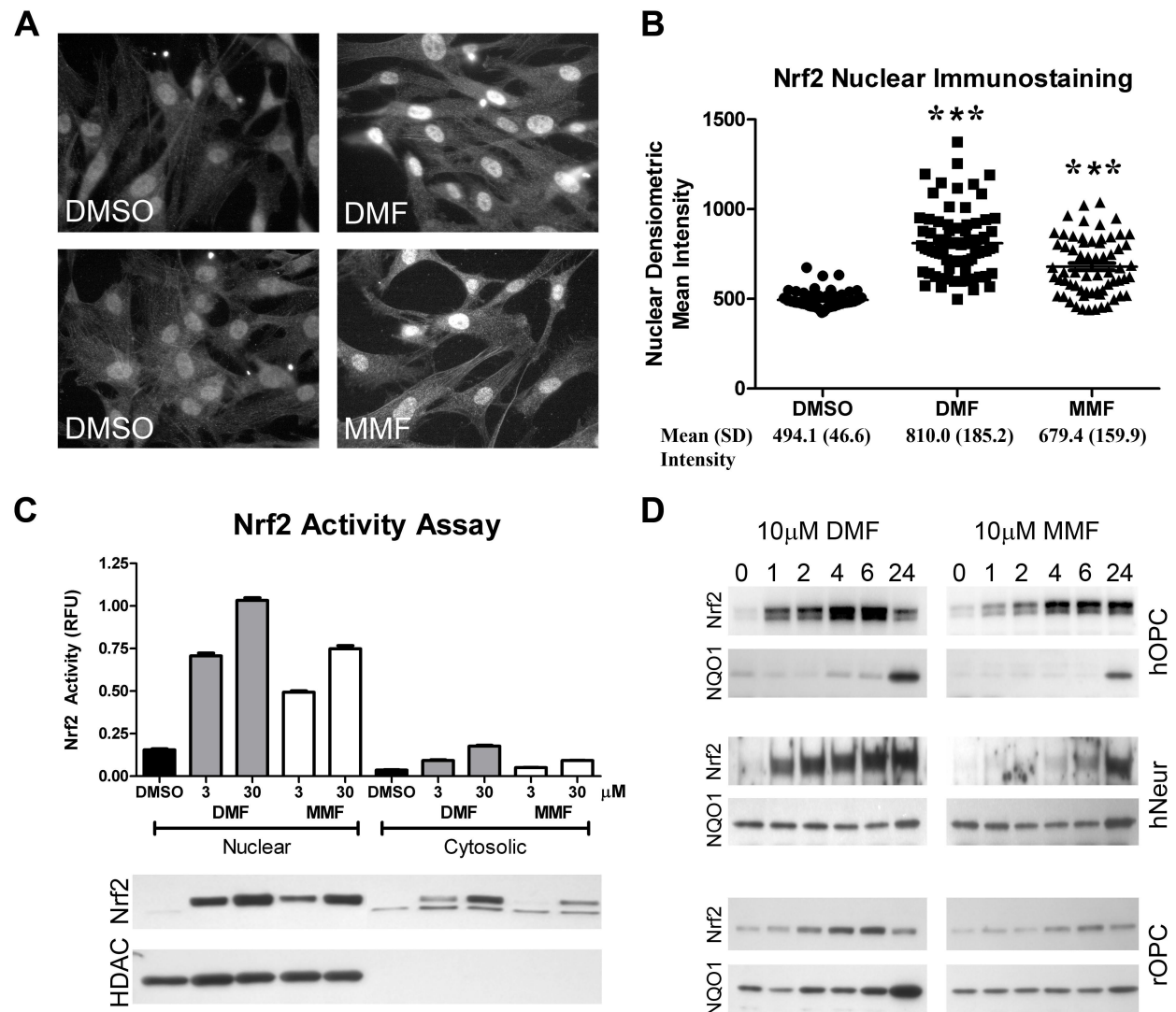


Figure 3

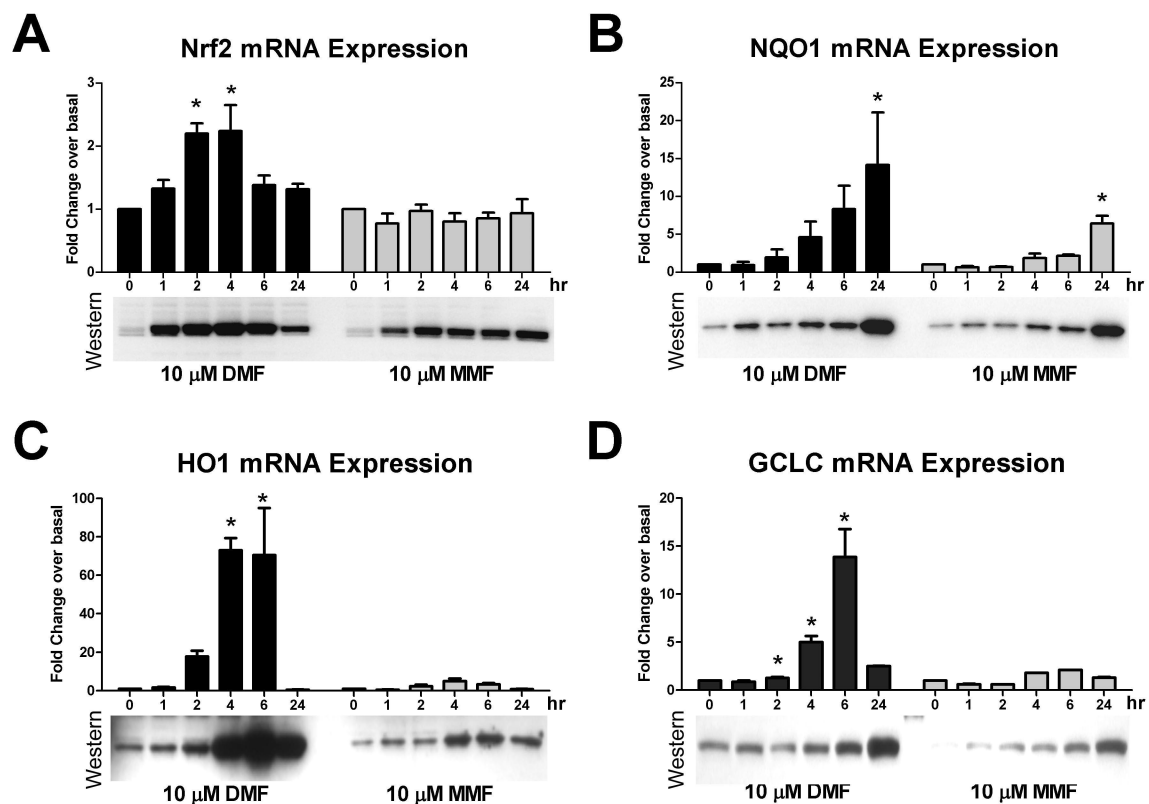


Figure 4

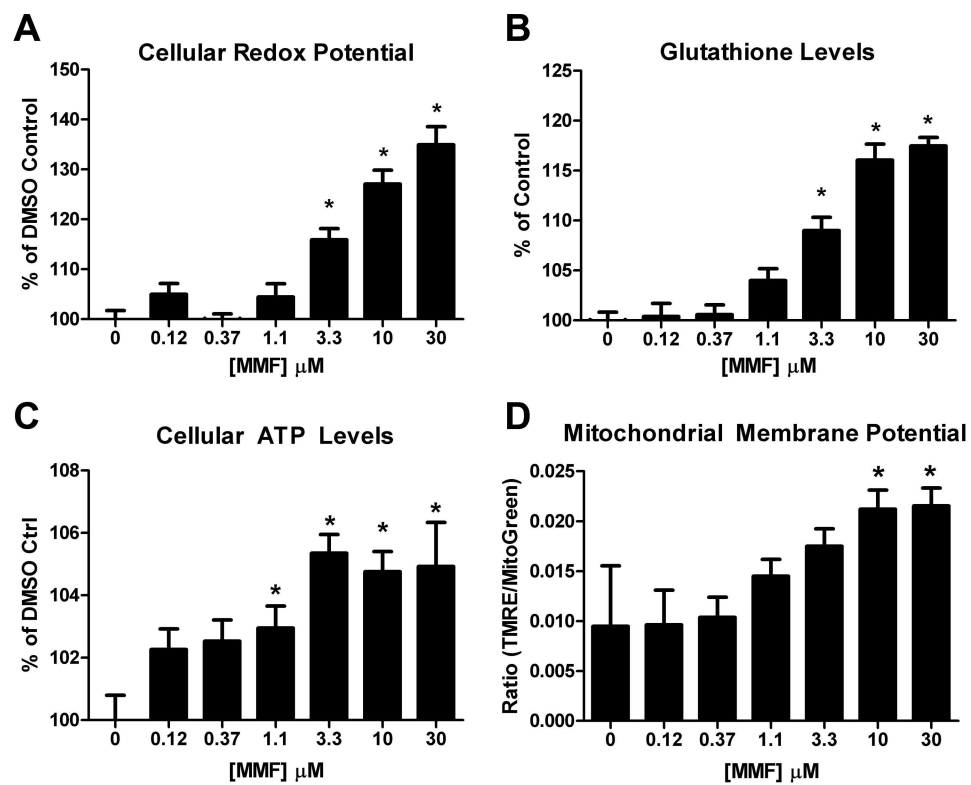


Figure 5

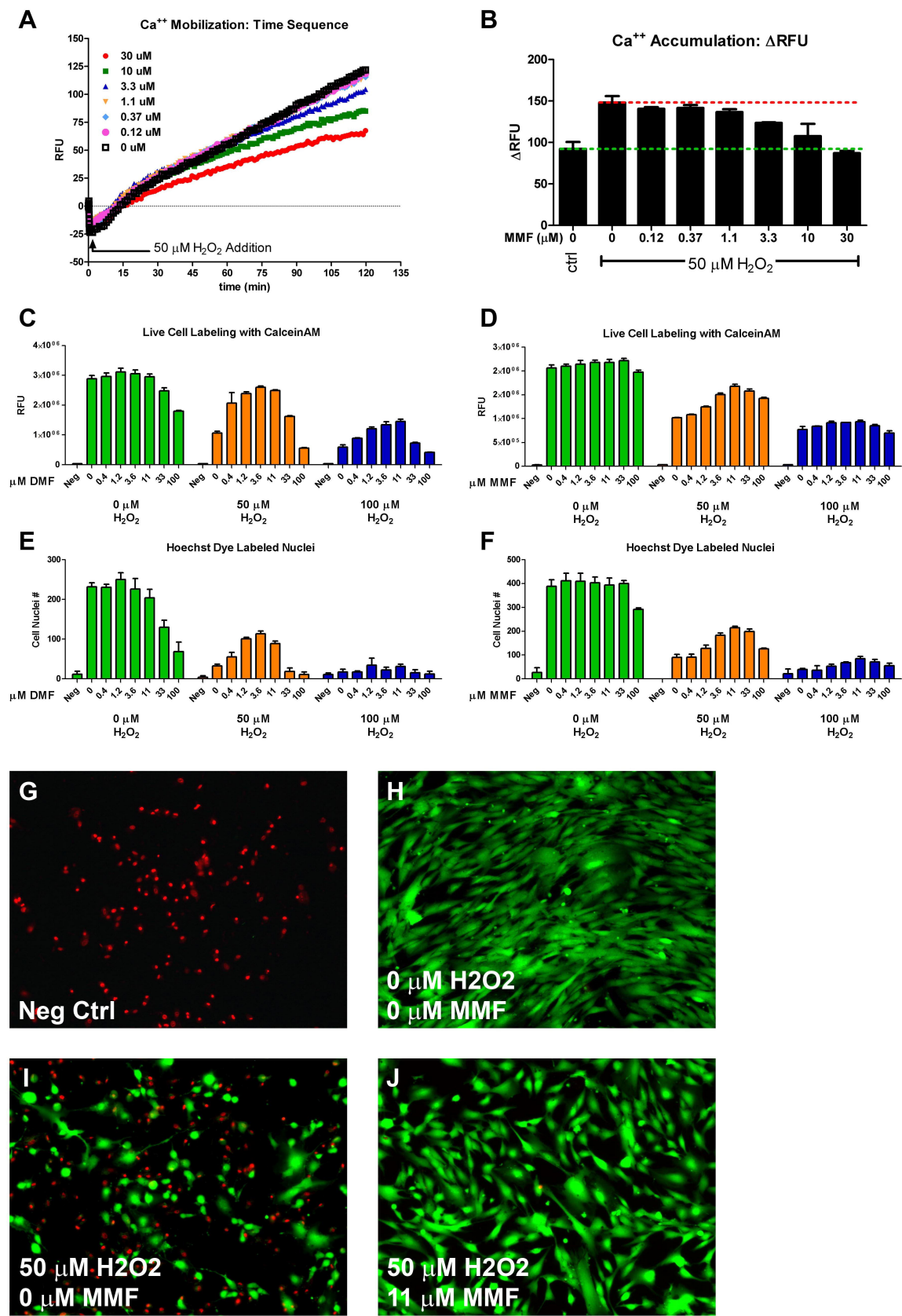


Figure 6

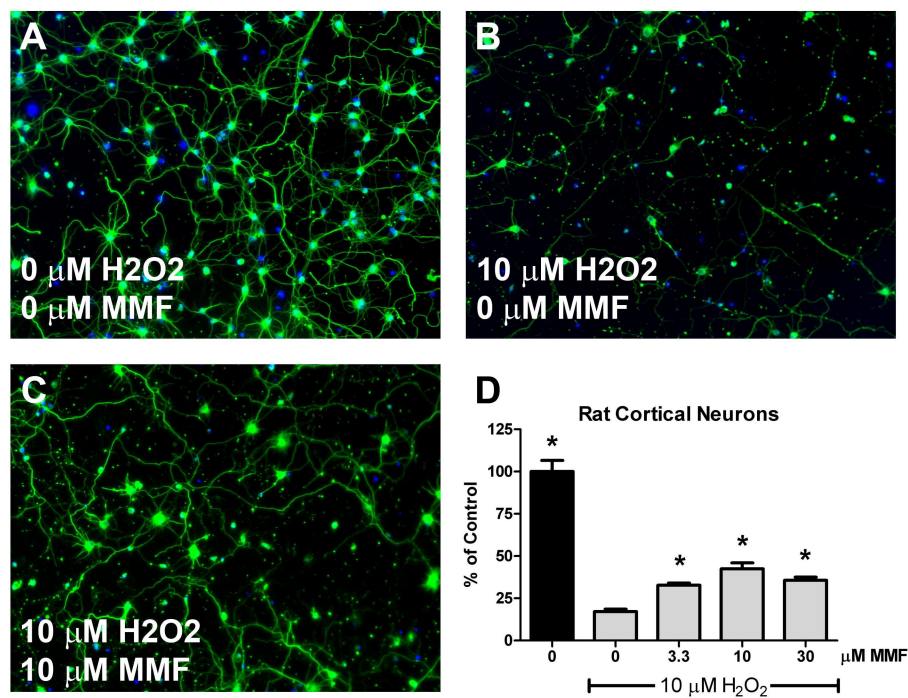


Figure 7

